

# Feasible Products for Kinetically Controlled Reactive Distillation of Ternary Mixtures

Nitin Chadda, Michael F. Malone, and Michael F. Doherty

Dept. of Chemical Engineering, University of Massachusetts, Amherst, MA 01003

*A method to determine feasible product compositions from a single-feed reactive distillation column for finite rates of reaction is presented. Tracking of pinch points to estimate the limit at minimum reflux is combined with performance modeling for the limit at the minimum number of stages. Using two examples it is shown how the product composition regions deform from the known limit of no reaction through intermediate rates of reaction and finally collapse onto the chemical equilibrium curve at extremely fast reaction rates. However, compositions can be achieved at intermediate reaction rates that do not lie between the limits for slow (no reaction) and fast (chemical equilibrium) reactions.*

## Introduction

The design of reactive distillation systems requires a knowledge of product composition specifications that will generate a feasible column design. In the absence of a method to determine the feasible product specifications, the design process, for example, by simulation is inefficient or impossible. Frequently, a feasible column design is only found when one or more of the product composition specifications is relaxed, leaving open the question of whether the originally desired specifications were feasible. To overcome this problem, feasibility analysis can be used to find the regions of the composition space that are accessible to reaction and separation by distillation.

Estimation of feasible distillates and bottoms regions for staged reactive distillation columns can be divided into three cases on the basis of the rate of reaction in the column: extremely slow rates of reaction (no reaction limit); intermediate rates of reaction (kinetic regime); and very fast reaction (chemical equilibrium limit).

Feasibility studies at the two extreme limiting cases are available. At the limit of no reaction two different approaches for the calculation of the feasible product regions are available. The first approach by Van Dongen (1983) and Van Dongen and Doherty (1985) used the similarity between the composition profiles in a distillation column and simple distillation residue curves at total reflux to estimate the feasible product regions, also referred to as the "bow-tie" regions. Stichlmair and Herguijuela (1992) proposed a similar method

that bounds the product compositions at total reflux. Wahnshafft et al. (1992) and Fidkowski et al. (1993) used a pinch tracking method to calculate the feasible distillates and bottoms in conventional distillation. The pinch-tracking methods are more accurate because they use the staged distillation column model equations and incorporate finite reflux ratios.

At the opposite limit of chemical equilibrium, Ung and Doherty (1995) introduced the concept of transformed composition variables to assess the feasibility for multiple equilibrium chemical reactions undergoing sharp splits in simple columns. Espinosa et al. (1995) used the transformed composition variables along with the pinch-tracking techniques to estimate the feasible product regions.

However, little is known about the feasible product regions at intermediate rates of reaction. The aim of this study is to estimate the product regions for ternary systems at intermediate rates of reaction and hence connect the known limits of no reaction and chemical equilibrium. We discuss a hybrid approach for the purpose of identifying feasible regions—pinch-tracking techniques to determine the limit at minimum reflux, and performance modeling to estimate the limit at the minimum number of stages. We will demonstrate that these limits encompass the feasible products for a given feed composition and rate of reaction.

## Feasible Product Regions at the Limiting Cases

Consider a liquid phase reaction



Correspondence concerning this article should be addressed to M. F. Doherty.

which is carried out in an ideal mixture with a rate given by

$$r_1 = k_f \left( x_3^2 - \frac{x_1 x_2}{K} \right), \quad (2)$$

where  $x_1$ ,  $x_2$ ,  $x_3$  are liquid-phase mol-fractions of  $A$ ,  $B$ , and  $C$ , respectively.  $A$  is the lightest boiling and  $B$  is the heaviest boiling component (the relative volatilities are  $\alpha_{AB}=5$  and  $\alpha_{CB}=3$ );  $k_f$  is the forward reaction-rate constant; and  $K$  is the chemical-equilibrium constant. We take  $K=0.25$  to be independent of temperature.

We consider a single-feed column, a total condenser, a partial reboiler, and that the reaction occurs on all stages including the condenser and the reboiler. We also assume the following:

(I) The column is adiabatic.

(II) The heat of vaporization is constant (independent of composition and temperature).

(III) The heats of mixing are negligible.

(IV) The heat of reaction is negligible compared to the enthalpy of vaporization.

(V) The feed is a saturated liquid.

These assumptions simply allow us to demonstrate the approach with the greatest clarity, and may be relaxed for many systems of practical interest.

Fidkowski et al. (1993) described an algorithm for estimating feasible product regions for the limit of no reaction. Applying this algorithm to the ternary system just described for a saturated liquid feed of  $x_F = (0.1, 0.1, 0.8)$ , we calculate the product regions as shown in Figure 1a. The only column designs possible are those for which the product specifications lie within the shaded areas.

At the other limit of chemical equilibrium (extremely fast reaction), we know that the feasible product compositions lie on the chemical equilibrium curve, as shown in Figure 1b. Barbosa (1989) and Espinosa et al. (1995) studied this limit and predicted the feasible product regions using transformed composition variables.

Comparison of Figures 1a and 1b suggests the following question: What are the feasible product regions at any intermediate rate of reaction, and how do the product distribution regions change/deform as we move away from the limit of no reaction through intermediate rates of reaction and finally reach the chemical-equilibrium limit?

The answer to this question is the object of this article.

## Distillation Limits and Feasibility

The feasible-product regions for an intermediate rate of reaction are encompassed by two bounds that are the distillation limit at minimum reflux and the distillation limit at the minimum number of stages. In this section we demonstrate the development of these bounds and show that these bounds limit that region of the composition space that is accessible to separation by reactive distillation.

### Distillation limit at minimum reflux

The overall mass balance for a reactive distillation column and the ternary reactive mixture in Eq. 1 can be written in terms of transformed variables given by Ung and Doherty

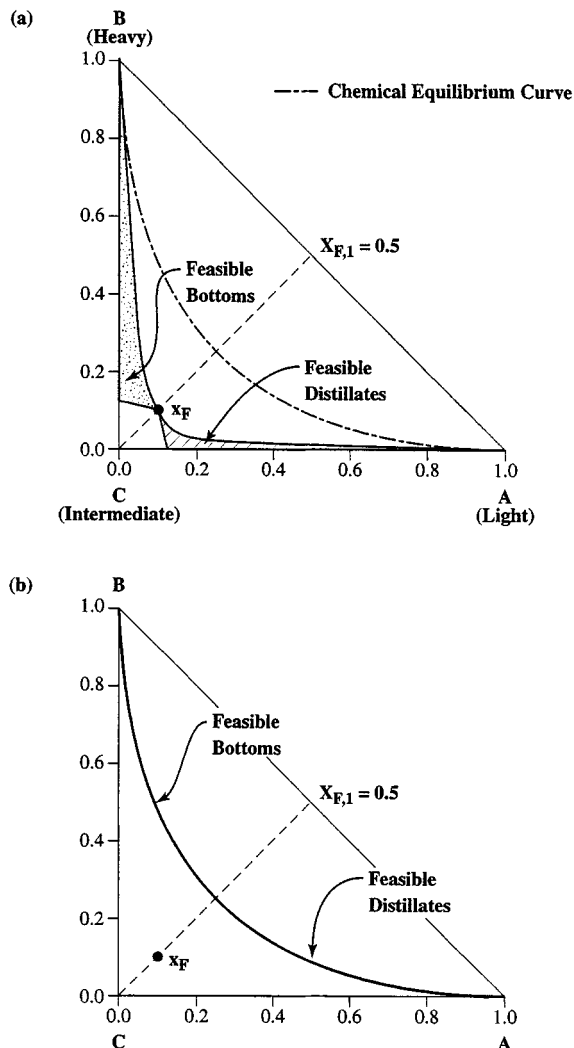


Figure 1. Feasible distillate and bottoms product regions at: (a)  $Da=0$  (no reaction limit) using Fidkowski's (1993) algorithm for a constant volatility ternary mixture given by Eq. 1 with  $x_F = (0.1, 0.1, 0.8)$ ; (b)  $Da=\infty$  (chemical equilibrium limit) for the system given by Eq. 1.

(1995):

$$\frac{D}{B} = \left( \frac{X_{F,1} - X_{B,1}}{X_{D,1} - X_{F,1}} \right), \quad (3)$$

where  $X_{F,1}$ ,  $X_{D,1}$  and  $X_{B,1}$  are transformed mol fractions for the feed, distillate, and the bottoms. Equation 3 is analogous to the lever rule for nonreactive systems in terms of mol fractions (Julka and Doherty, 1990). The transformed mol fractions defined by Ung and Doherty (1995) can be written for a single chemical reaction as follows:

$$X_i = \left( \frac{x_i \nu_k - x_k \nu_i}{\nu_k - \nu_T x_k} \right), \quad (i = 1, 2) \quad (4)$$

where  $k$  is the reference component.

For our system we choose component 3 as the reference component. Using the definition given in Eq. 4, the transformed mol fractions can then be written as

$$\begin{aligned} X_1 &= x_1 + 0.5x_3 \\ X_2 &= x_2 + 0.5x_3. \end{aligned} \quad (5)$$

From Eq. 5, the sum of the two transformed mol fractions is unity (Ung and Doherty, 1995). Thus, only one of the transformed composition variables is independent. We choose  $X_1$  as the independent variable. It is clear that the transformed mol fraction,  $X_1 = 0$  implies  $x_1 = 0$  and  $X_1 = 1$  implies  $x_1 = 1$ . However,  $X_1$  does not generally specify  $x_1$ , for example, when  $X_1 = 0.95$ ,  $x_1$  ranges from 0.90 to 0.95.

The advantage of transformed variables is that they help reduce the dimensionality of the problem in the limit of chemical-reaction equilibrium. In addition, these reaction invariant variables can be used to write the lever rule in transformed mol fraction coordinates (Eq. 3). For our example, which is a three-component system with a single reaction, the mol-fraction space is two-dimensional ( $0 \leq x_1 \leq 1$ ;  $0 \leq x_2 \leq 1$ ) for the no-reaction limit and for finite rates of reaction (kinetic regime). However, at chemical equilibrium, the solution space is just the transformed composition line ( $0 \leq X_1 \leq 1$ ). In the kinetic regime, although the problem is represented in the mol fraction space, the overall mass balance is still satisfied by the lever rule in transformed mole fractions (Eq. 3). We will therefore make use of both ordinary as well as transformed mol fractions to estimate the two distillation limits in the kinetic regime.

Equation 3 can be rewritten as

$$\left(\frac{D}{B}\right)X_{D,1} + X_{B,1} = \left(\frac{D}{B} + 1\right)X_{F,1}. \quad (6)$$

For a given pure reactant  $C$  feed ( $X_{F,1} = 0.5$ ), and  $D/B = 1$ , Eq. 6 becomes

$$X_{D,1} + X_{B,1} = 1.0. \quad (7)$$

We can choose different ( $X_{D,1}$ ,  $X_{B,1}$ ) pairs that satisfy this overall mass balance, for example,  $X_{D,1} = 0.7$  and  $X_{B,1} = 0.3$ . For  $x_{B,1}$  lying on  $X_{B,1} = 0.3$  we can find all feasible values of  $x_{D,1}$  lying on  $X_{D,1} = 0.7$  using the "Boundary Value Design Procedure" given in Buzad and Doherty (1995). The rectifying and stripping section design equations used there have been modified slightly to account for a revised definition of the Damköhler number ( $Da$ ).

Rectifying section design equations ( $m$  stages)

$$\begin{aligned} y_{m+1,i} - \left(\frac{r}{r+1}\right)x_{m,i} - \left(\frac{1}{r+1}\right)x_{Di} + \left(\frac{1+\frac{B}{D}}{r+1}\right)\left(\frac{k_f}{k_{f,\text{ref}}}\right) \\ \times Da \sum_{j=1}^m \left(x_{j,3}^2 - \frac{x_{j,1}x_{j,2}}{K}\right) = 0 \quad (i=1,2). \end{aligned} \quad (8)$$

Stripping section design equations ( $n$  stages)

$$\begin{aligned} x_{n+1,i} - \left(\frac{s}{s+1}\right)y_{n,i} - \left(\frac{1}{s+1}\right)x_{Bi} + \left(\frac{1+\frac{D}{B}}{s+1}\right)\left(\frac{k_f}{k_{f,\text{ref}}}\right) \\ \times Da \sum_{j=1}^n \left(x_{j,3}^2 - \frac{x_{j,1}x_{j,2}}{K}\right) = 0 \quad (i=1,2). \end{aligned} \quad (9)$$

In Eqs. 8 and 9 the Damköhler number is defined as the ratio of a characteristic residence time to a characteristic reaction time (Damköhler, 1939):

$$Da = \left(\frac{H/F}{1/k_{f,\text{ref}}}\right), \quad (10)$$

where  $H$  is the molar liquid holdup on a stage (assumed equal on all stages),  $F$  is the molar feed flow rate to the column, and  $k_{f,\text{ref}}$  is the forward rate constant evaluated at a reference temperature,  $T_{\text{ref}}$ . For this example we have chosen  $k_f$  to be independent of temperature, thus implying that  $k_f/k_{f,\text{ref}} = 1$ .

The reflux ratio ( $r$ ) and the reboil ratio ( $s$ ) are not independent of each other. An overall energy balance for a saturated liquid feed with constant molar flows (implied the first four assumptions together with an equimolar reaction) links them together by

$$\frac{D}{B} = \left(\frac{s}{r+1}\right). \quad (11)$$

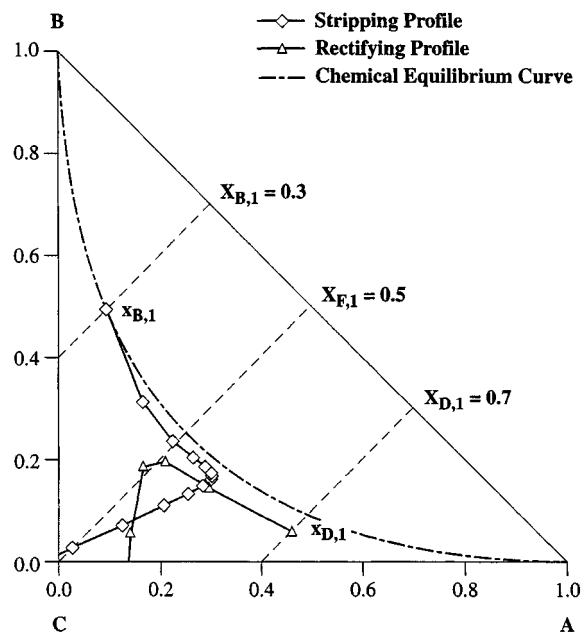


Figure 2. Typical feasible reactive column design for a saturated liquid pure-reactant feed and  $Da = 0.1305$ .

Product specifications:  $x_{D,1} = 0.46$ ,  $X_{D,1} = 0.7$ ,  $x_{B,1} = 0.0885$ ,  $X_{B,1} = 0.3$ .

Figure 2 shows composition profiles and a feasible design for the reactive system given by Eq. 1 at  $Da=0.1305$ . The feed to the column is pure C, and the product specifications are as follows:  $x_{D,1}=0.46$ ,  $X_{D,1}=0.7$ ,  $x_{B,1}=0.0885$ ,  $X_{B,1}=0.3$ . The resulting column design has 14 stages and a reflux ratio of 0.935.

Keeping the bottoms composition fixed at the same value as in Figure 2, we search for all possible feasible column designs with the distillate compositions along  $X_{D,1}=0.7$ , both above and below  $x_{D,1}=0.46$ . Figure 3 shows the limiting column profiles for  $x_{B,1}=0.0885$ ,  $X_{B,1}=0.3$ , and  $X_{D,1}=0.7$ . The point  $x_{D,1}^U$  in Figure 3a corresponds to the largest value of  $x_{D,1}$  for the given  $x_{B,1}$ . It represents the starting point of a rectifying profile that contains a saddle pinch (a pinch point is a fixed point of Eqs. 8 and 9 that is approached asymptotically closely by the column profile; for a discussion of the behavior and properties of fixed points of the staged reactive distillation model used here, see Buzad and Doherty (1994) and Appendix A in this article),  $\hat{x}_r$ , and just touches the stripping profile that originates at  $x_{B,1}$ . In similar fashion,

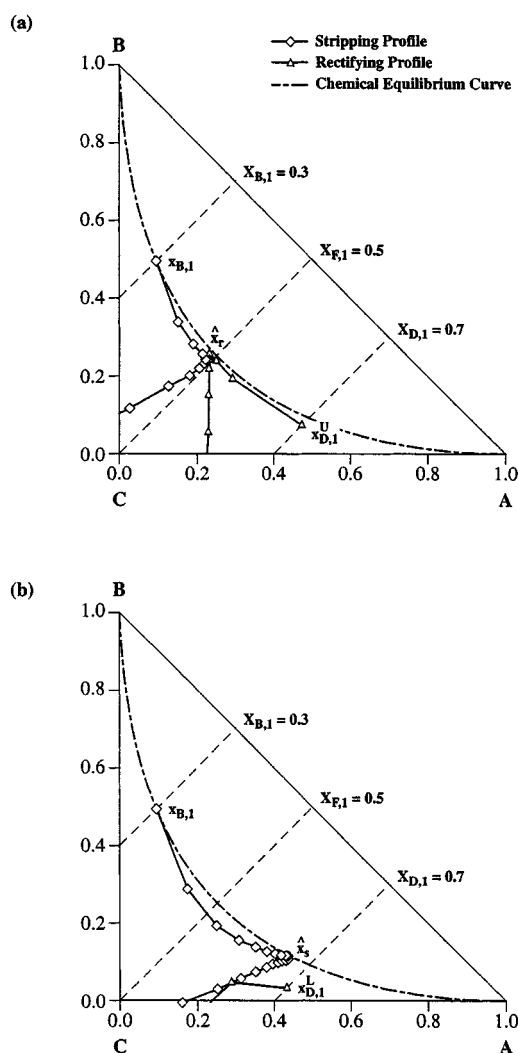


Figure 3. Limiting distillates on  $X_{D,1}=0.7$  corresponding to  $x_{B,1}=0.0885$  and  $X_{B,1}=0.3$  at  $Da=0.1305$  for a saturated liquid reactant feed.

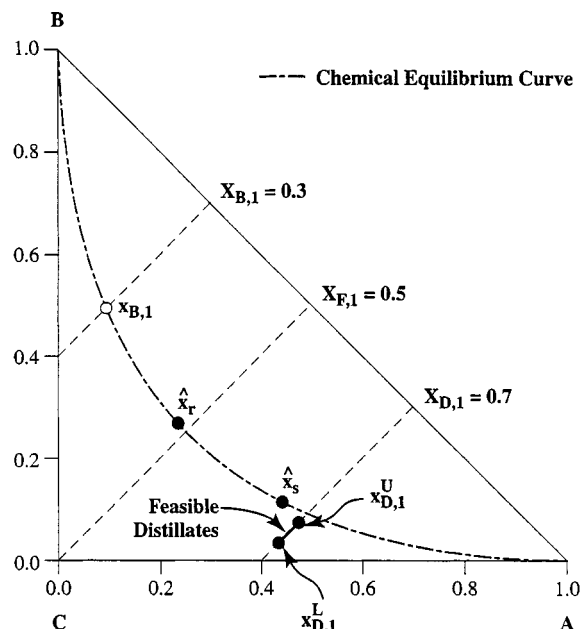


Figure 4. Distillate region on  $X_{D,1}=0.7$  corresponding to  $x_{B,1}=0.0885$  and  $X_{B,1}=0.3$  at  $Da=0.1305$  for a saturated liquid reactant feed.

the point  $x_{D,1}^L$  in Figure 3b corresponds to the smallest value of  $x_{D,1}$  lying on  $X_{D,1}$ . It represents the starting point of the rectifying profile that just touches the stripping profile that originates at  $x_{B,1}$  and contains a saddle pinch,  $\hat{x}_s$ . The region along  $X_{D,1}=0.7$  between  $x_{D,1}^U$  and  $x_{D,1}^L$  represents all possible feasible distillates for the given  $x_{B,1}$  and is shown in Figure 4. The rectifying profiles originating from distillate compositions within this region and the stripping profiles originating at  $x_{B,1}$  will satisfy the criteria for a feasible reactive column design, which are

1. Intersection of the rectifying and stripping profiles (as in distillation without chemical reaction);
2. The total extent of a reaction in the column as given by the overall mass balance must equal the sum of extents of the reaction on all stages in the rectifying and stripping sections, as well as the condenser and reboiler.

As we move along  $X_{D,1}$  from  $x_{D,1}^U$  to  $x_{D,1}^L$  (for a fixed value of  $x_{B,1}$ ), the values of the reflux ratio for which feasible designs occur lie between  $r=0.266$  and  $r=2.01$ . A plot of  $N_T$  vs.  $r$  for feasible column designs having distillate compositions between  $x_{D,1}^U$  and  $x_{D,1}^L$  and bottoms composition fixed at  $x_{B,1}=0.0885$  and  $X_{B,1}=0.3$  is shown in Figure 5. The column design at  $r=0.266$  corresponds to a large number of stages in the rectifying section at the rectifying saddle pinch,  $\hat{x}_r$ , with the stripping profile just barely touching it. As the reflux ratio increases, the rectifying profile moves away from the rectifying pinch and the number of stages decreases until it reaches a minimum. Further increase in the reflux ratio leads to the stripping profile beginning to pinch at the stripping pinch causing the number of stages to rise again. Finally, at  $r=2.01$  there is a large number of stages in the stripping section at the stripping pinch,  $\hat{x}_s$ , with the rectifying profile barely touching it. A similar plot was also reported by

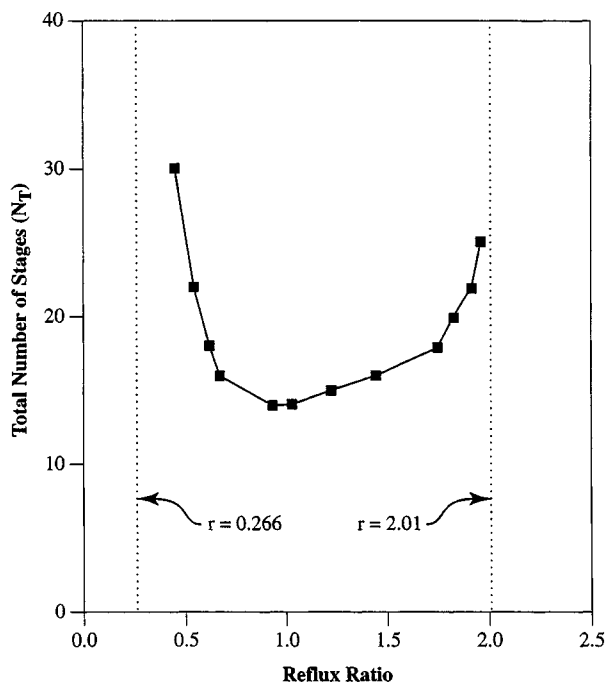


Figure 5. Total number of stages vs. reflux ratio.

Data points are individual feasible designs for a saturated liquid reactant feed. Specifications:  $X_{D,1} = 0.7$ ,  $x_{B,1} = 0.0885$  and  $X_{B,1} = 0.3$ ,  $Da = 0.1305$ .

Okasinski and Doherty for a different  $(X_{D,1}, X_{B,1})$  pair and  $Da$  (Okasinski and Doherty, 1998, Figure 3).

As  $x_{B,1}$  increases along  $X_{B,1}$ , the rectifying and stripping saddle pinches ( $\hat{x}_r$  and  $\hat{x}_s$ , respectively) start to approach each other along the reaction equilibrium curve. Correspondingly, the distillate region on  $X_{D,1}$  (that is, the region between  $x_{D,1}^L$  and  $x_{D,1}^U$ ) decreases in width, shifts toward the equilibrium curve, and overlaps the previous region. Ultimately, a limit is reached where for a particular value of  $x_{B,1}$  the rectifying and stripping pinches coalesce ( $\hat{x}_r = \hat{x}_s$ ) on the transformed feed composition line at the feed stage and a unique distillate composition,  $x_{D,1}^*$  lying on  $X_{D,1}$ , corresponds to a single bottoms composition,  $x_{B,1}^*$  lying on  $X_{B,1}$ . The limiting points  $x_{D,1}^*$  and  $x_{B,1}^*$  lie on the distillation limit at minimum reflux ratio, as shown in Figure 6. This geometric condition (coalescence of the rectifying and stripping pinches on the transformed feed mol fraction line) can be exploited to derive a simple analytical expression for the minimum reflux ratio for a given  $(X_{D,1}, X_{B,1})$  pair.

$$r_{\min} + 1 = \left( \frac{X_{D,1} - X_{F,1}}{Y_{F,1} - X_{F,1}} \right), \quad (12)$$

where,  $Y_{F,1}$  is in simultaneous phase and chemical equilibrium, with  $X_{F,1}$  the transformed feed mol fraction. The derivation is provided in Appendix B.

Once the minimum reflux ratio is calculated for a given  $(X_{D,1}, X_{B,1})$  pair using Eq. 12, the problem of determining the distillate (bottoms) compositions on the distillation limit reduces to a one-variable numerical search. This is to determine the value of  $x_{D,1}$  ( $x_{B,1}$ ) that will give a rectifying (stripping) profile with a pinch on the transformed feed mol frac-

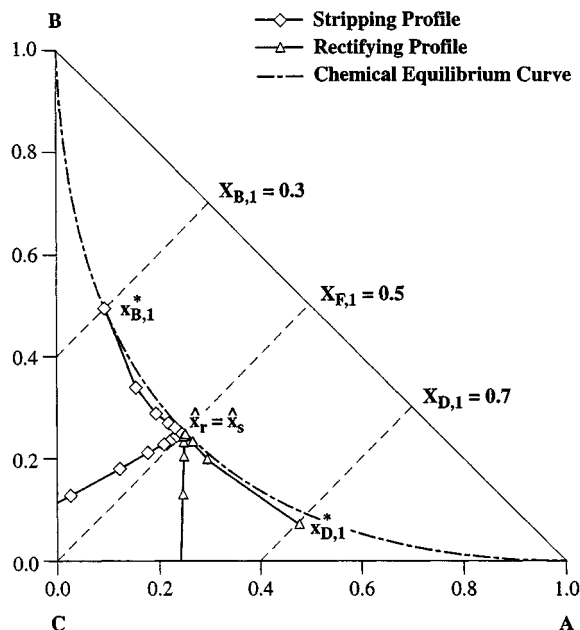


Figure 6. Distillate and bottoms compositions at minimum reflux for  $Da = 0.1305$ .

tion,  $X_{F,1}$  using Eq. 8 (Eq. 9). These special product composition points are denoted by  $x_{D,1}^*$  and  $x_{B,1}^*$ . For our example,  $X_{D,1} = 0.7$ ,  $X_{B,1} = 0.3$ ,  $Da = 0.1305$ , the minimum reflux ratio is  $r_{\min} = 0.2$  as calculated from Eq. 12. Using this value, we search for  $x_{D,1}^*$  (lying on  $X_{D,1} = 0.7$ ) and  $x_{B,1}^*$  (lying on  $X_{B,1} = 0.3$ ) using Eqs. 8 and 9. These limiting points are shown in Figure 6. The other points on the distillation limit at  $D/B = 1$  can be similarly determined by using different  $(X_{D,1}, X_{B,1})$  pairs that satisfy the overall mass balance (Eq. 7). The result is shown in Figure 7.

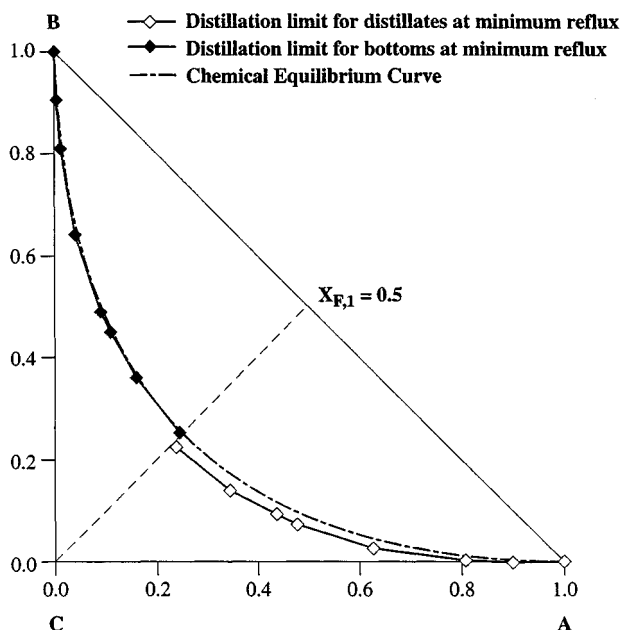


Figure 7. Distillation limit at minimum reflux for  $D/B = 1$  for  $Da = 0.1305$ .

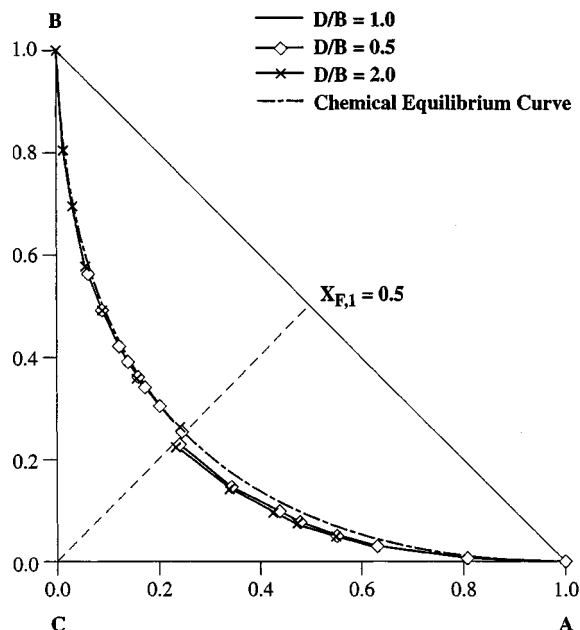


Figure 8. Distillation limits at minimum reflux for different  $D/B$  ratios for  $Da=0.1305$ .

We can similarly estimate the distillation limits at minimum reflux ratio for different values of  $D/B$  with the result shown in Figure 8. It is clear from the figure that the distillation limit is virtually independent of  $D/B$ . For our example, which has  $X_{F,1} = 0.5$ ,  $D/B = 1$  implies that  $0 \leq X_{B,1} \leq 0.5$  and  $0.5 \leq X_{D,1} \leq 1$ . Thus, we can “sweep” the entire transformed composition line  $0 \leq X_1 \leq 1$ . Any other value of  $D/B$  would indicate that  $X_{D,1}$  and  $X_{B,1}$  only partially sweep the transformed composition line. Therefore, it is convenient to use the value of  $D/B = 1$  for computing the distillation limit at minimum reflux ratio. For a different  $X_{F,1}$ , the  $D/B$  that sweeps the entire transformed composition line will be different. This value of  $D/B$  is obtained by equating the righthand side of Eq. 6 to unity.

The distillation limit at minimum reflux ratio is a function of the transformed feed mol fraction  $X_{F,1}$ . All feed-composition mol fractions,  $x_{F,1}$  lying on  $X_{F,1}$  will yield the same distillation limit. Of course, the distillation limit at minimum reflux ratio also depends on  $Da$ .

#### Distillation limit at minimum number of stages

In the previous section we showed that as  $x_{B,1}$  increases from the value in Figure 2 along  $X_{B,1} = 0.3$ , the corresponding distillate region on  $X_{D,1} = 0.7$  shrinks until the condition shown in Figure 6 is reached, corresponding to the minimum reflux case. In this subsection we investigate what happens when  $x_{B,1}$  is decreased from the value in Figure 2 along  $X_{B,1} = 0.3$ .

When we decrease  $x_{B,1}$  along  $X_{B,1} = 0.3$ , the rectifying and stripping pinch points (lying on the chemical equilibrium curve) start to move away from each other. Correspondingly, the distillate region lying on  $X_{D,1} = 0.7$  increases in size from that shown in Figure 4. A situation arises when, for a given value of  $x_{B,1}$ , the stripping fixed point moves outside the col-

umn, that is, it lies on the transformed mol fraction,  $X_1 > X_{D,1}$ . The total number of stages vs. reflux ratio for  $x_{B,1} = 0.0485$  and an overall mass balance governed by the (0.7, 0.3) pair at  $Da = 0.1305$  is shown in Figure 9a. A typical feasible column design corresponding to  $r = 17$  in Figure 9a is shown in Figure 9b. The design has a finite number of stages and it can be seen that the stripping fixed point is located outside the column beyond  $X_{D,1} = 0.7$ . Comparing Figures 5 and 9a, we make the following observation. In Figure 5, for  $x_{B,1} = 0.0885$  the distillate region is bounded by designs at an infinite number of stages (corresponding to the rectifying and stripping pinches). However, in Figure 9a, for  $x_{B,1} = 0.0485$

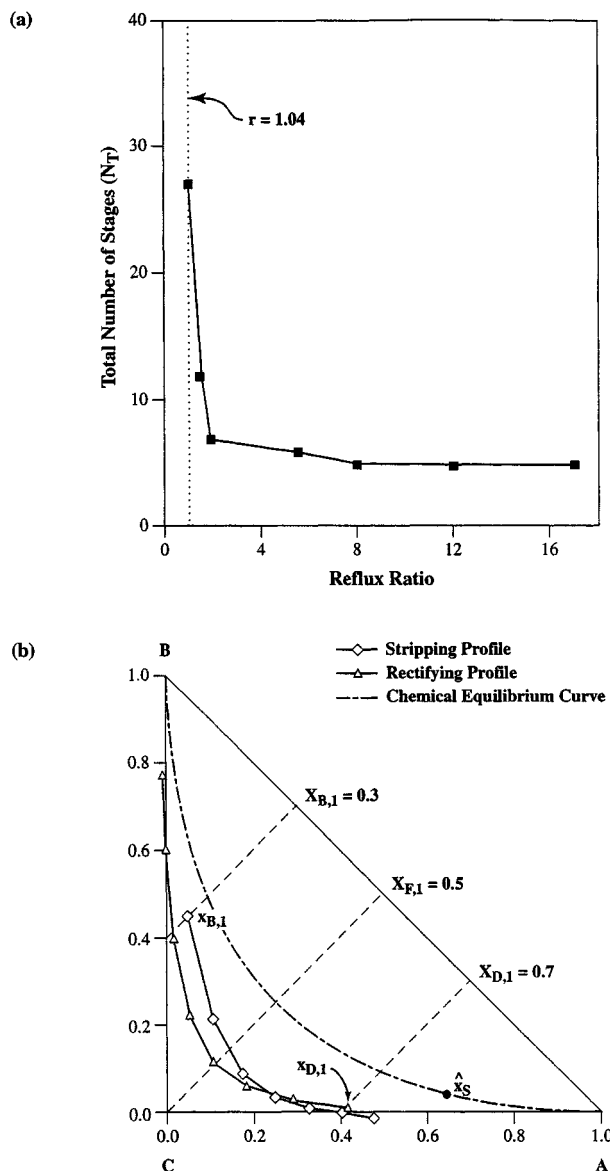


Figure 9. (a) Total number of stages vs. reflux ratio at  $Da=0.1305$ ; (b) typical feasible reactive column design with stripping fixed point outside the column.

For (a), data points are individual designs for a saturated liquid reactant feed. Specifications:  $X_{D,1} = 0.7$ ,  $x_{B,1} = 0.0485$  and  $X_{B,1} = 0.3$ . For (b), design at  $r = 17$  in Figure 9a.

the distillate region is bounded by designs at an infinite number of stages (due to the rectifying pinch) and a finite number of stages (due to the absence of stripping pinch in the column). This indicates that as  $x_{B,1}$  decreases along  $X_{B,1} = 0.3$ , the lower limit of the feasible distillate composition (lying on  $X_{D,1} = 0.7$ ), which was previously determined by an infinite number of stages, is now determined by a finite number of stages. We conclude that as  $x_{B,1}$  decreases further along  $X_{B,1} = 0.3$ , there will be a minimum number of stages that will satisfy the overall mass balance given by the (0.7, 0.3) pair. The distillate and bottoms compositions that satisfy this condition will lie on the distillation limit at a minimum number of stages.

We determine this distillation limit at a minimum number of stages from a performance calculation. The five degrees of freedom specified for the simulation are  $Da$ ,  $D/B$ ,  $N_T$ , feed location, and  $r$ . For a pure reactant feed and  $D/B = 1$ , the distillate and bottoms composition are constrained to lie on  $(X_{D,1}, X_{B,1})$  pairs that satisfy the overall mass balance given by Eq. 7, for example, (0.7, 0.3). The idea here is to simulate and find a column design using the minimum number of stages with the constraint that the distillate and bottoms compositions lie on  $X_{D,1} = 0.7$  and  $X_{B,1} = 0.3$ , respectively.

To accomplish this, we start with the smallest number of stages in the column, which is one, and by simulation determine if it is possible to satisfy the overall mass balance for any value of reflux ratio. If the number of stages is insufficient, we increase the number of stages by one until the overall mass balance is first satisfied. For example, the minimum number of stages for the overall mass balance given by the (0.7, 0.3) pair and  $Da = 0.1305$  is 4 (including the reboiler), as shown in Figure 10. The value of the reflux ratio is 31.02, which is the maximum achievable value of reflux ratio for the (0.7, 0.3) pair at  $D/B = 1$ . The distillate ( $x_{D,1}^+$ ) and bottoms compositions ( $x_{B,1}^+$ ) are the product-composition mol fractions lying on the *distillation limit at minimum number of stages* for the pair (0.7, 0.3) at  $D/B = 1$ . An increase or decrease in the reflux ratio (keeping the number of stages fixed at 4) will lead to product compositions that do not obey the overall mass balance given by the (0.7, 0.3) pair.

An increase in the number of stages (with a simultaneous decrease in reflux ratio to satisfy the overall mass balance) will make the distillate ( $x_{D,1}$ ) and bottoms compositions ( $x_{B,1}$ ) move away from  $x_{D,1}^+$  and  $x_{B,1}^+$  along  $X_{D,1} = 0.7$  and  $X_{B,1} = 0.3$ , respectively, until they reach  $x_{D,1}^*$  and  $x_{B,1}^*$ , respectively, which lie on the distillation limit at minimum reflux ratio. A decrease in the number of stages from the minimum, however, will lead to distillate and bottoms compositions that do not satisfy the overall mass balance given by the (0.7, 0.3) pair.

Other points on the distillation limit at a minimum number of stages at  $D/B = 1$  can be estimated using  $(X_{D,1}, X_{B,1})$  pairs satisfying Eq. 7. In similar fashion we can estimate the distillation limits at a minimum number of stages for different values of  $D/B$  ratios. These are shown in Figure 11. We notice that unlike the distillation limit at minimum reflux ratio, the distillation limit at a minimum number of stages is dependent on the  $D/B$  ratio. To account for this variability, we calculate a distillation limit that is an outer locus of all product compositions at a minimum number of stages as a function of  $D/B$ . This limit is shown in Figure 12. A step-by-step procedure

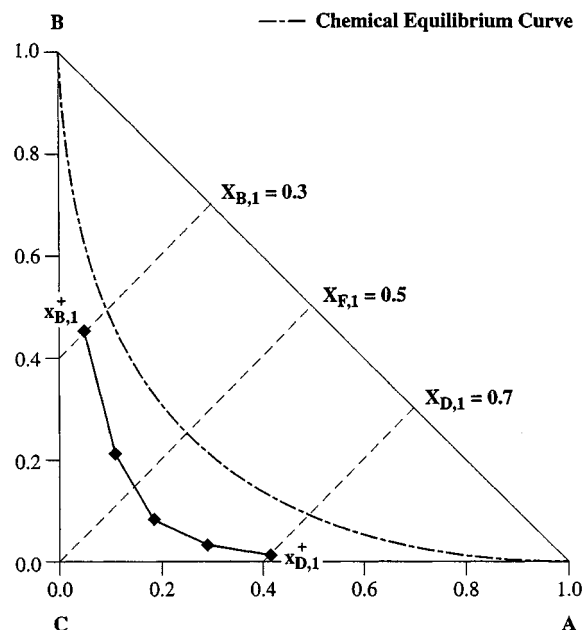


Figure 10. Distillate and bottoms composition at minimum number of stages for an overall mass balance.

Simulation degrees of freedom:  $N_T = 4$ , feed stage = 2,  $r = 31.02$ ,  $D/B = 1$ ,  $Da = 0.1305$ .

describing the calculation of this limit at a minimum number of stages that takes into account the variation in  $D/B$  is provided in step (2) of the feasibility algorithm described in the next section.

Like the distillation limit at minimum reflux ratio, the distillation limit at a minimum number of stages is also de-

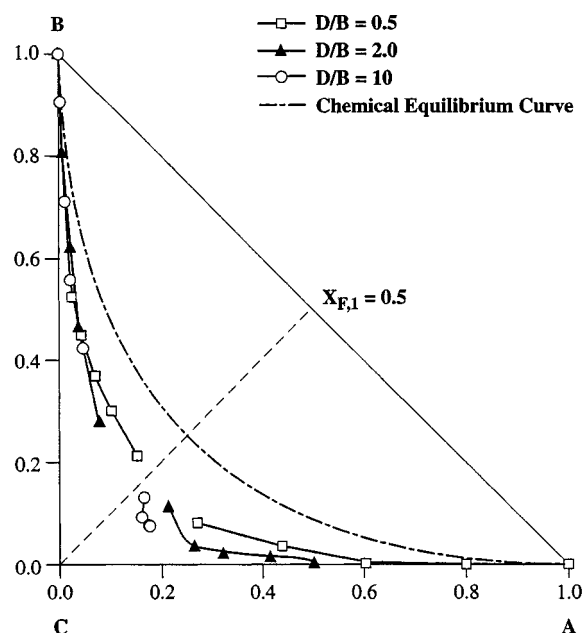


Figure 11. Distillation limits at minimum number of stages for different  $D/B$  ratios at  $Da = 0.1305$ .

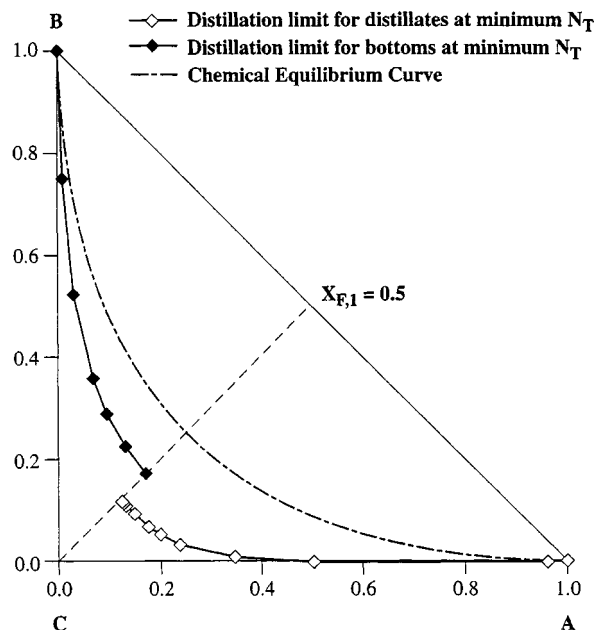


Figure 12. Distillation limit at minimum number of stages at  $Da=0.1305$  for a saturated liquid reactant feed taking into account the variation with respect to the  $D/B$  ratio.

pendent on  $Da$ . However, it depends on the feed composition,  $x_{F,1}$ , unlike the distillation limit at minimum reflux ratio, for which all  $x_{F,1}$  that lie on the same transformed feed mol fraction,  $X_{F,1}$ , have the same distillation limit.

### Feasibility Algorithm

The overall procedure for the calculation of the feasibility distillates and bottoms regions for the reactive distillation of ternary mixtures is provided in the algorithm below. For a given saturated liquid feed composition, column pressure, and Damköhler number, there are two bounds on the feasible regions: the distillation limit at minimum reflux ratio, and the distillation limit at a minimum number of stages. Further, the feasible distillates region is separated from the feasible bottoms region by the transformed feed mol fraction line. This algorithm is applicable to those ternary systems for which the branches of saddle pinches for the rectifying and stripping sections overlap each other along the chemical equilibrium curve. Chemistries of the form as given by Eq. 1, and so on, satisfy this condition and can be treated by this algorithm.

#### Step (1): Distillation limit at minimum reflux ratio

- Calculate  $X_{F,1}$  from the feed-composition mol fractions using Eq. 4.
- Calculate  $Y_{F,1}$  from a bubble point calculation using  $P$  and  $x_F$ .
- Determine  $D/B$  by equating the righthand side of Eq. 6 to unity.
- Select  $X_{D,1}$  close to 1 (such as 0.99).
- Calculate  $X_{B,1}$  using Eq. 6.
- Determine the minimum reflux ratio for this  $(X_{D,1}, X_{B,1})$  pair using Eq. 12.

(vii) Calculate the corresponding reboil ratio from Eq. 11.

(viii) Numerically solve Eqs. 8 and 9 to determine the location of the distillate,  $x_{D,1}^*$  and bottoms composition,  $x_{B,1}^*$  (with the constraint that they lie on  $X_{D,1}$  and  $X_{B,1}$ , respectively). This will make the rectifying and stripping saddle pinches coalesce on the intersection of the transformed feed mol fraction line and the equilibrium curve (as in Figure 6).

(ix) Repeat steps (v) through (viii) for different values of  $X_{D,1}$  less than 1.0 but greater than  $X_{D,1}^0$  at which  $r_{\min} = 0$ .

(x) For  $X_{F,1} \leq X_{D,1} < X_{D,1}^0$ , the minimum reflux ratio is negative. Since we exceed the distillate specification with a value of  $r \leq 0$ , use  $r = 0$  for calculation of the distillate composition lying on the distillation limit. Calculate the corresponding value of  $s$  from the energy balance (Eq. 11). Next, using Eq. 8 (and 9) calculate the distillate (and bottoms) compositions lying on  $X_{D,1}$  (and  $X_{B,1}$ ) which would give a saddle pinch on the chemical equilibrium curve at  $r = 0$  (and  $s$ ).

(xi) Join all the distillates ( $x_{D,1}^*$ ) and the bottoms compositions ( $x_{B,1}^*$ ) so obtained. The result is the distillation limit at minimum reflux ratio.

#### Step (2): Distillation limit at minimum number of stages

This distillation limit is calculated with the help of a simulator. We determine the distillate and bottoms distillation limits separately as shown below.

(a) *Limit for Distillates.* This is the locus of all distillate compositions lying on the maximum possible transformed distillate mol fraction for a particular  $D/B$  ratio (called  $X_{D,1}^{\max}$ ).

(i) Select a  $D/B$  between the value calculated in step 1 (ii) and  $\infty$  (such as 10).

(ii) Calculate  $X_{D,1}^{\max}$  for this  $D/B$  ratio by putting  $X_{B,1} = 0$  in Eq. 6, that is,

$$X_{D,1}^{\max} = X_{F,1} \left( 1 + \frac{1}{D/B} \right). \quad (13)$$

(iii) Specify the four remaining degrees of freedom for the simulation:  $N_T$ ,  $r = \text{very large}$  (say 10,000),  $Da$ , feed stage = top stage (simulations have shown that to include all possible column designs for a minimum number of stages, the distillation limit at minimum number of stages for the distillates should be calculated with the feed stage as the top stage; likewise, the distillation limit at a minimum number of stages for the bottoms must be calculated with the feed stage as the last stage) [Note:  $D/B$  is the fifth degree of freedom, which is already specified in step (i)].

(iv) Using the simulator, find the minimum number of stages necessary to satisfy the overall mass balance as given by Eq. 13 for the selected  $D/B$ . Start with one stage and check whether the overall balance will be satisfied. If not, increase the number of stages by one and repeat the process. Continue until the overall mass balance as given by the  $(X_{D,1}^{\max}, 0)$  pair is first satisfied. Make a note of the distillate composition,  $x_{D,1}^+$ .

(v) Repeat steps (i) through (iv) for different  $D/B$ .

(vi) Join all  $x_{D,1}^+$  so obtained. The result is the distillation limit at a minimum number of stages for the distillates.

(b) *Limit for Bottoms.* This is the locus of all bottoms compositions lying on the minimum possible transformed



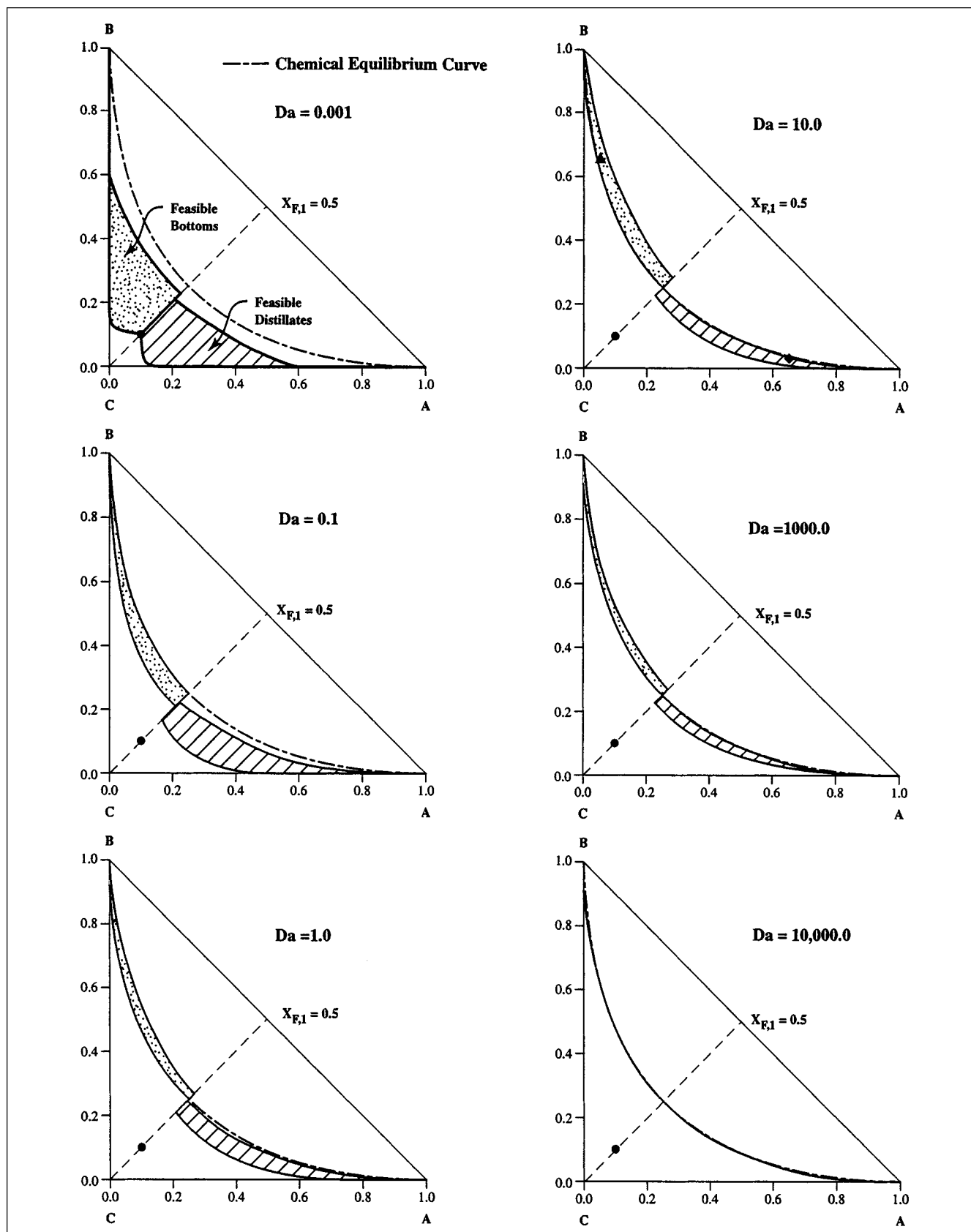


Figure 13. Feasible distillate and bottoms product regions at various values of  $Da$  for Example 1:  $x_F = (0.1, 0.1, 0.8)$  marked by •.

bottoms mol fraction for a particular  $D/B$  ratio (called  $X_{B,1}^{\min}$ ).

(i) Select a  $D/B$  between 0 and the value calculated in step 1 (ii) (such as 0.1).

(ii) Calculate  $X_{B,1}^{\min}$  for this  $D/B$  ratio by putting  $X_{D,1} = 1$  in Eq. 6, that is,

$$X_{B,1}^{\min} = X_{F,1} \left( 1 + \frac{D}{B} \right) - \frac{D}{B}. \quad (14)$$

(iii) Specify the four remaining degrees of freedom for the simulation:  $N_T$ ,  $s$  = very large (say 10,000),  $Da$ , feed stage = bottom stage.

(iv) Using the simulator find the minimum number of stages necessary to satisfy the overall mass balance as given by Eq. 14 for the selected  $D/B$ . Start with one stage and check whether the overall balance will be satisfied. If not, increase the number of stages by one and repeat the simulation. Continue until the overall mass balance as given by the (1,  $X_{B,1}^{\min}$ ) pair is first satisfied. Make a note of the bottoms composition,  $x_{B,1}^+$ .

(v) Repeat steps (i) through (iv) for different  $D/B$  ratios.

(vi) Join all  $x_{B,1}^+$  so obtained. The result is the distillation limit at the minimum number of stages for the bottoms.

### Steps (3): Transformed feed mol fraction line

Draw the line  $X_1 = X_{F,1}$  on the mole-fraction composition triangle. The feasible distillates are separated from the feasible bottoms by the transformed mol fraction feed line,  $X_1 = X_{F,1}$ . This is due to the fact that  $X_{F,1}$  must lie between  $X_{B,1}$  and  $X_{D,1}$  from the lever rule in Eq. 3.

## Examples

In this section, we apply the algorithm from the previous section to determine the feasible product regions for two examples.

### Example 1

Here we consider the constant volatility ternary system given by Eq. 1. The feed composition is  $x_F = (0.1, 0.1, 0.8)$  and is a saturated liquid. The feasible product regions for various values of  $Da$  are shown in Figure 13. An important result is that pure A and pure B can be obtained as products irrespective of the rate of reaction.

The feasible product regions deform smoothly as  $Da$  is increased from a very small value ( $Da = 0.001$ ) to a large value ( $Da = 10,000$ ). At a larger value the two distillation limits are essentially superimposed on the chemical equilibrium curve. This is the limit of chemical equilibrium where all column composition profiles lie on the chemical-equilibrium curve and the dimensionality of the problem is reduced by one. The kinetic product regions converge on the equilibrium product regions as  $Da$  gets large. This limit of chemical equilibrium has been studied in more detail by other authors, notably Barbosa and Doherty (1988), Ung and Doherty (1995), and Espinosa et al. (1995).

For values of  $Da > \sim 0.5$ , an interesting phenomenon occurs. The feasible bottoms region lies on the opposite side of chemical-equilibrium curve to the feed composition. As  $Da$  increases, the distillation limit for the bottoms at a minimum

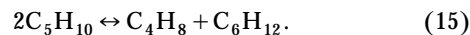
number of stages moves further away from the chemical-equilibrium curve, and it is farthest from the chemical-equilibrium curve at  $Da = 10$ . Any further increase in  $Da$  brings the distillation limit back toward the equilibrium curve until it collapses onto the equilibrium curve at large  $Da$ . To verify that this prediction is not a numerical artifact, we simulated reactive columns for a variety of inputs (feed compositions) and parameters ( $N_T$ , feed stage location,  $Da$ ,  $r$ ,  $s$ ) and found that the outputs (distillate and bottoms compositions) do in fact lie inside the feasible regions, even when they fall on the "wrong" side of the chemical-equilibrium curve. For example, Figure 13 for  $Da = 10$ , shows the distillate and bottoms compositions achievable with the following inputs and parameters:  $x_F = (0.1, 0.1, 0.8)$ ,  $N_T = 5$ , feed stage = 2,  $r = 39$ , and  $s = 40$ . The distillate and bottoms compositions are shown by a filled diamond and a filled triangle, respectively. It is noteworthy that the bottoms composition lies on the "wrong" side of the chemical-equilibrium curve, as predicted by the feasibility algorithm.

At the other end of the reaction-rate spectrum, that is, at  $Da = 0$  (no reaction limit), Fidkowski et al. (1993) have proposed an algorithm for the estimation of the feasible product regions in ternary mixtures. For the same system and feed composition as in this example, and using Fidkowski's algorithm, the feasible product regions at  $Da = 0$  are shown in Figure 1a. We immediately notice that there is a visible difference in the feasible regions between  $Da = 0$  and  $Da = 0.001$  shown in Figure 13. This can be attributed to a singular limit at  $Da = 0$ . For example, at  $Da = 0$ , for a given distillate and bottoms composition lying on the  $AC$  and  $BC$  edges of the triangular composition diagram and a finite reflux and reboil ratio, respectively, the saddle pinches of the rectifying and stripping profiles lie on the  $AC$  and  $BC$  edges of the triangular composition diagram, respectively. However, the moment we turn on the reaction even slightly ( $Da = 0.001$ ), these saddle pinches move discontinuously onto the chemical-equilibrium curve, thereby causing the rapid distortion of feasible product regions between  $Da = 0$  and  $Da = 0.001$ . This happens because, although at  $Da = 0.001$  the holdup on a stage is finite (and small), the total holdup in the column with a saddle pinch will be infinite because of the infinite number of stages. At infinite total holdup, we have conditions of chemical reaction equilibrium at the pinch, thereby causing the saddle pinch to lie on the chemical-equilibrium curve.

A way of getting around this problem would be to redefine  $Da$  on the basis of a fixed and finite total molar holdup in a column and to reformulate the column model. This total holdup model is discussed in Appendix C. However, its usefulness in estimating the feasible product regions is limited, as explained in this appendix.

### Example 2

Here, we consider the metathesis of 2-pentene to 2-butene and 3-hexene



The reaction occurs at atmospheric pressure and has negligible heat of reaction. The temperature range for reactive

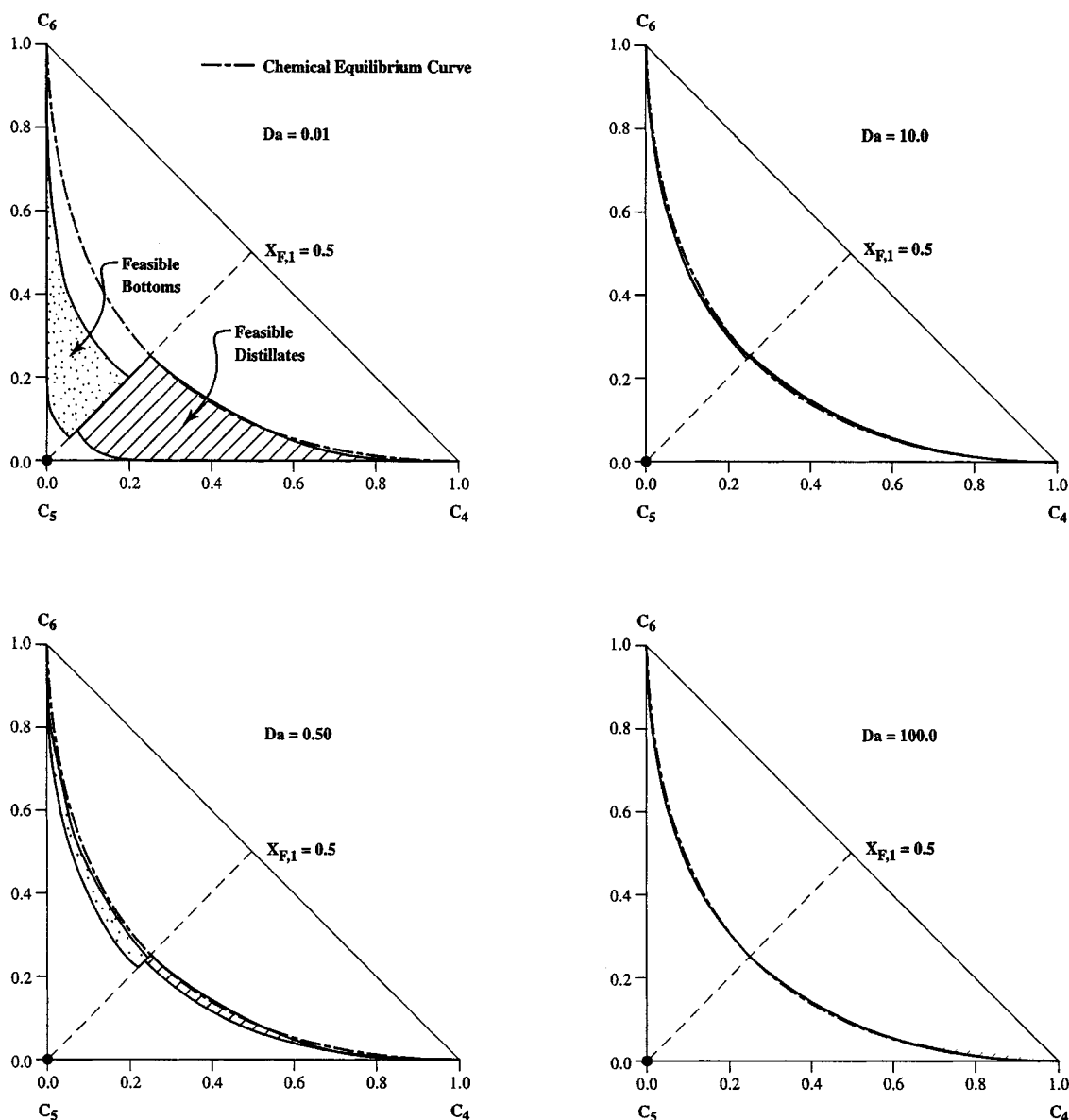


Figure 14. Feasible distillate and bottoms product regions at various values of  $Da$  for Example 2:  $x_F = (0, 0, 1)$  marked by •.

distillation operation is  $4^\circ\text{C} < T < 67^\circ\text{C}$ . The system has an ideal vapor–liquid equilibrium. Physical property data and kinetic rate expression have been taken from Okasinski and Doherty (1998). 2-Butene was chosen as the reference component. The temperature-dependent rate expression is given by

$$r_{C_6} = 0.5k_f \left( x_{C_5}^2 - \frac{x_{C_4}x_{C_6}}{K} \right), \quad (16)$$

where  $k_f = 3,553.6 e^{(-6.6[\text{kcal/mol}]/RT)} \text{ min}^{-1}$  and  $K = 0.25$ .

Figure 14 shows the feasible product regions for this system at different  $Da$  for a saturated liquid feed of pure 2-pentene. The feasible product regions distort smoothly with  $Da$  and collapse onto the chemical-equilibrium curve at large  $Da$ .

## Conclusion

Feasible product regions for the reactive distillation of ternary systems with negligible heats of reaction are determined by a systematic procedure. This provides an estimate of the product regions at intermediate rates of reaction that are accessible by reactive distillation. It was shown that the rectifying and stripping profiles originating from the distillate and bottoms compositions that lead to saddle pinch points coalescing on the transformed feed mol fraction line lie on the distillation limit at minimum reflux ratio. The distillation limit at a minimum number of stages was calculated with the aid of a simulator. These two bounds help distinguish the feasible product compositions from the infeasible product compositions in the mol fraction composition space. An algorithm was developed to estimate the feasible product regions of ternary systems for a given feed composition. The algo-

rithm is applicable to those ternary systems for which the branches of saddle fixed points for the rectifying and stripping sections overlap each other along the reaction equilibrium curve. The application of the algorithm was illustrated in two examples, including the metathesis of 2-pentene to 2-butene and 3-hexene. An important result is that 2-butene and 3-hexene can be obtained as products irrespective of the rate of reaction.

## Acknowledgment

We are grateful for financial support from the National Science Foundation (grant number CTS-9613489). We are also grateful to Dr. Fengrong Chen for help in adapting his simulation program to the constant volatility mixture. We also acknowledge Ms. Pam Stephan for her drafting services.

## Notation

$B$  = bottoms product flow rate, mol/time  
 $c$  = number of components  
 $D$  = distillate flow rate, mol/time  
 $k_{f,\text{ref}}$  = forward reaction rate constant at the reference temperature  
 $\nu_i$  = stoichiometric coefficient for component  $i$   
 $\nu_T$  = summation of all stoichiometric coefficients  
 $N_T$  = total number of stages in the column  
 $R$  = universal gas constant

## Subscripts and Superscripts

$j$  = stage index  
 $m$  = stage index for rectifying section  
 $n$  = stage index for stripping section  
 $s$  = stripping section  
 $*$  = product composition at minimum reflux  
 $L$  = lower bound  
 $r$  = rectifying section  
 $t$  = product composition at minimum number of stages  
 $U$  = upper bound

## Literature Cited

- Barbosa, D., and M. F. Doherty, "Design and Minimum Reflux Calculations for Single-Feed Multicomponent Reactive Distillation Columns," *Chem. Eng. Sci.*, **43**, 1523 (1988).  
 Barbosa, D., "Analytical Expressions for the Calculation of Minimum Reflux Ratio for Ternary Reactive Distillation Columns," Unpublished report, Univ. of Massachusetts, Amherst, MA (1989).  
 Buzad, G., and M. F. Doherty, "Design of Three-Component Kinetically Controlled Reactive Distillation Columns Using Fixed-Point Methods," *Chem. Eng. Sci.*, **49**, 1947 (1994).  
 Buzad, G., and M. F. Doherty, "New Tools for the Design of Kinetically Controlled Reactive Distillation Columns for Ternary Mixtures," *Comput. Chem. Eng.*, **19**, 395 (1995).  
 Damköhler, G., "Stromungs und Wärmeübergangsprobleme in Chemischer Technik," *Chem. Ing. Tech.*, **12**, 469 (1939).  
 Espinosa, J., P. A. Aguirre, and G. A. Perez, "Product Composition Regions of Single-Feed Reactive Distillation Columns: Mixtures Containing Inerts," *Ind. Eng. Chem. Res.*, **34**, 853 (1995).  
 Fidkowski, Z. T., M. F. Doherty, and M. F. Malone, "Feasibility of Separations for Distillation of Nonideal Ternary Mixtures," *AIChE J.*, **39**, 1303 (1993).  
 Huan, S., and K. M. Lien, "A Phenomena Based Design Approach to Reactive Distillation," *Trans. Inst. Chem. Eng.*, **76**, 396 (1998).  
 Julka, V., and M. F. Doherty, "Geometric Behavior and Minimum Flows for Nonideal Multi-Component Distillation," *Chem. Eng. Sci.*, **45**, 1801 (1990).  
 Okasinski, M. J., and M. F. Doherty, "Design Method for Kinetically Controlled, Staged Reactive Distillation Columns," *Ind. Eng. Chem. Res.*, **37**, 2821 (1998).  
 Stichlmair, J. G., and J. R. Fair, "Separation Regions and Processes of Zeotropic and Azeotropic Ternary Distillation," *AIChE J.*, **38**, 1523 (1992).

- Stichlmair, J. G., and J. R. Fair, *Distillation Principles and Practices*, Wiley-VCH (1998).  
 Ung, S., and M. F. Doherty, "Synthesis of Reactive Distillation Systems with Multiple Equilibrium Chemical Reactions," *Ind. Eng. Chem. Res.*, **34**, 2555 (1995).  
 Van Dongen, D. B., "Distillation of Azeotropic Mixtures: The Application of Simple Distillation Theory to Design of Continuous Processes," PhD Diss., Univ. of Massachusetts, Amherst, MA (1983).  
 Van Dongen, D. B., and M. F. Doherty, "Design and Synthesis of Homogeneous Azeotropic Distillations: 1. Problem Formulation for a Single Column," *Ind. Eng. Chem. Fundam.*, **24**, 454 (1985).  
 Venimadhavan, G., M. F. Malone, and M. F. Doherty, "Bifurcation Study of Kinetic Effects in Reactive Distillation," *AIChE J.*, **45**, 546 (1999).  
 Wahnschafft, O. M., J. W. Koehler, E. Blass, and A. W. Westerberg, "The Product Composition Regions of Single-Feed Azeotropic Distillation Columns," *Ind. Eng. Chem. Res.*, **31**, 2345 (1992).

## Appendix A

The fixed points of the rectifying and stripping sections always lie on the reaction equilibrium curve.

The operating line for an envelope of  $n$  stages in the stripping section is given by Eq. 9. For an envelope of  $(n-1)$  stages, the corresponding stripping operating line will be

$$x_{n,i} - \left( \frac{s}{s+1} \right) y_{n-1,i} - \left( \frac{1}{s+1} \right) x_{Bi} + \left( \frac{1 + \frac{D}{B}}{s+1} \right) \left( \frac{k_f}{k_{f,\text{ref}}} \right) \times Da \sum_{j=1}^{n-1} \left( x_{j,3}^2 - \frac{x_{j,1} x_{j,2}}{K} \right) = 0 \quad (i=1, 2). \quad (\text{A1})$$

Subtracting Eq. A1 from Eq. 9, we get

$$(x_{n+1,i} - x_{n,i}) - \left( \frac{s}{s+1} \right) (y_{n,i} - y_{n-1,i}) + \left( \frac{1 + \frac{D}{B}}{s+1} \right) \times \left( \frac{k_f}{k_{f,\text{ref}}} \right) Da \left( x_{n,3}^2 - \frac{x_{n,1} x_{n,2}}{K} \right) = 0 \quad (i=1, 2). \quad (\text{A2})$$

At a fixed point,  $(x_{n+1,i} - x_{n,i}) \rightarrow 0$  as  $n \rightarrow \infty$ , which implies that  $(y_{n,i} - y_{n-1,i}) \rightarrow 0$  as  $n \rightarrow \infty$ . Therefore, at a fixed point,  $\hat{x}$ , Eq. A2 reduces to

$$\left( \hat{x}_3^2 - \frac{\hat{x}_1 \hat{x}_2}{K} \right) = 0. \quad (\text{A3})$$

This implies that the fixed points of the stripping section will always lie on the chemical-equilibrium curve.

For a general chemistry, the equivalent fixed-point criteria can be obtained in accordance with the model described earlier. The equivalent of Eq. A2 for a general chemistry is given by

$$[(V_n + B)x_{n+1,i} - (V_n + B)x_{n,i}] - [V_n y_{n,i} - V_{n-1} y_{n-1,i}] = Da \cdot F \left[ (\nu_i - \nu_T x_{n+1,i}) \sum_{j=1} R(\mathbf{x}_j) - (\nu_i - \nu_T x_{n,i}) \sum_{j=1}^{n-1} R(\mathbf{x}_j) \right] \quad (i=1, 2), \quad (\text{A4})$$

where  $F$  is the feed flow to the column;  $V_n$  is the vapor flow out of the  $n$ th stage; and  $R(\mathbf{x}_j)$  is the driving force for the reaction on the  $j$ th stage. For example, a chemistry of the type given by Eq. 1 has an  $R(\mathbf{x}_j)$  given by

$$R(\mathbf{x}_j) = \left( x_{j,3}^2 - \frac{x_{j,1} x_{j,2}}{K} \right). \quad (\text{A5})$$

Next, we introduce a new parameter,  $D$  (Venimadhavan et al., 1999), defined as

$$D = \frac{Da}{1 + Da}, \quad (\text{A6})$$

where  $D$  varies from 0 to 1 with  $D = 0$  being the no-reaction limit and  $D = 1$  the chemical-reaction equilibrium limit. Values of  $D$  intermediate between 0 and 1 represent the kinetic reaction regime. The advantage of this parametric formulation is that it avoids a singular limit at chemical equilibrium where  $Da = \infty$  and  $R(\mathbf{x}) = 0$ . Incorporating Eq. A6 into Eq. A5 gives us the following equation:

$$\begin{aligned} & (1 - D)[(V_n + B)x_{n+1,i} - (V_n + B)x_{n,i}] \\ & - (1 - D)[V_n y_{n,i} - V_{n-1} y_{n-1,i}] \\ & = D \cdot F \left[ (\nu_i - \nu_T x_{n+1,i}) \sum_{j=1}^n R(\mathbf{x}_j) - (\nu_i - \nu_T x_{n,i}) \sum_{j=1}^{n-1} R(\mathbf{x}_j) \right] \\ & \quad (i = 1, 2). \quad (\text{A7}) \end{aligned}$$

The liquid and vapor flows do not change at a fixed point, nor do the liquid and vapor compositions. Thus at a fixed point we have the following condition:

$$\begin{aligned} V_n &= V_{n-1} = \hat{V} \\ x_{n+1} &= x_n = \hat{x} \\ y_n &= y_{n-1} = \hat{y}. \end{aligned} \quad (\text{A8})$$

Applying these conditions to Eq. A7, we get the criteria for the existence of fixed points

$$D(\nu_i - \nu_T \hat{x}_i) R(\hat{\mathbf{x}}) = 0 \quad (i = 1, 2). \quad (\text{A9})$$

Equation A9 tells us that for all  $0 < D \leq 1$ , one of the fixed points for the stripping map will always lie at the pole point,  $\hat{x}_i = \nu_i / \nu_T$  ( $i = 1, 2$ ) (Hauan and Lien, 1998; Stichlmair and Fair, 1998). All other fixed points lie on the chemical-equilibrium curve ( $R(\hat{\mathbf{x}}) = 0$ ).

It is known that the pole point always lies outside the physically realizable composition space and will thus never be a pinch point. However, fixed points that lie on the chemical-equilibrium curve in the interior of the physically realizable composition space have the potential to become pinch points, because stripping profiles can come asymptotically close to them. The location of these pinch points is independent of the operating reaction regime. For kinetic as well as chemical-equilibrium-limited regimes, the pinch points will always be located on the chemical-equilibrium curve.

A similar result is obtained for the rectifying section.

## Appendix B

*The rectifying and stripping saddle pinches coalesce at the intersection of the transformed feed mol fraction line and the chemical equilibrium curve at minimum reflux ratio.*

The criterion for the existence of fixed points of the rectifying map for a ternary system can be obtained by writing Eq. 8 for components 1 and 3 (reference component) and adding the two equations:

$$\hat{Y}_{r,1} = \left( \frac{r}{r+1} \right) \hat{X}_{r,1} + \left( \frac{1}{r+1} \right) X_{D,1}. \quad (\text{B1})$$

Likewise, for the stripping map, the criterion for the existence of fixed points is given by

$$\hat{X}_{s,1} = \left( \frac{s}{s+1} \right) \hat{Y}_{s,1} + \left( \frac{1}{s+1} \right) X_{B,1}, \quad (\text{B2})$$

with the restriction that the fixed points lie on the equilibrium curve (Buzad and Doherty, 1994 and Appendix A of this article). Equations A3 and B1 are the necessary and sufficient conditions for the existence of a fixed point in a rectifying map. Similarly, Eqs. A3 and B2 are the necessary and sufficient conditions for fixed points of a stripping map.

For the fixed points of the rectifying and stripping maps to coalesce,

$$\begin{aligned} \hat{X}_{s,1} &= \hat{X}_{r,1} = \hat{X}_1 \\ \hat{Y}_{s,1} &= \hat{Y}_{r,1} = \hat{Y}_1. \end{aligned} \quad (\text{B3})$$

Using Eqs. B3 in Eqs. B1 and B2, and eliminating  $\hat{Y}_1$ , we get

$$\hat{X}_1 = \left( \frac{sX_{D,1} + (r+1)X_{B,1}}{s+r+1} \right). \quad (\text{B4})$$

For a saturated liquid feed, the energy balance is given by Eq. 11. From Eqs. B4 and 11, eliminating  $r$  and  $s$  and rearranging, we get the following equation:

$$\frac{D}{B} = \left( \frac{\hat{X}_1 - X_{B,1}}{X_{D,1} - \hat{X}_1} \right). \quad (\text{B5})$$

The overall mass balance can also be written in terms of the transformed mol fractions, and is given by Eq. 3. Obviously, for Eq. 3 and Eq. B5 to be satisfied simultaneously,

$$\hat{X}_1 = X_{F,1}, \quad (\text{B6})$$

that is, the rectifying and stripping pinches must both be located at the intersection of the transformed feed mol fraction line and the chemical-equilibrium curve. Since  $\hat{Y}_1$  is in chemical equilibrium with  $\hat{X}_1$ , it follows from Eq. B6 that

$$\hat{Y}_1 = Y_{F,1}, \quad (\text{B7})$$

where  $Y_{F,1}$  is the transformed vapor composition in chemical equilibrium with  $X_{F,1}$ . These conditions are true for saturated liquid feeds, but can be extended to nonsaturated liquid feeds following similar arguments.

The value of the reflux ratio at which the two pinches coalesce on the transformed feed mol fraction line is the minimum reflux ratio and is calculated by making  $r$  the subject of the formula in Eq. B1:

$$r_{\min} + 1 = \left( \frac{X_{D,1} - \hat{X}_1}{\hat{Y}_1 - \hat{X}_1} \right). \quad (\text{B8})$$

Substituting Eqs. B6 and B7 into Eq. B8 gives Eq. 12.

## Appendix C

*The total holdup formulation.*

The model used throughout this study uses the definition of  $Da$  given by Eq. 10. This model formulation yields a singularity at  $Da=0$  as noted in Example 1. To avoid this singularity we can reformulate the model by defining  $Da$  as

$$Da = \left( \frac{H_T/F}{1/k_{f,\text{ref}}} \right), \quad (\text{C1})$$

where  $H_T$  is the total holdup of the reacting liquid in the column that is a fixed and finite quantity. The design equations for the rectifying and stripping sections become

$$y_{m+1,i} - \left( \frac{r}{r+1} \right) x_{m,i} - \left( \frac{1}{r+1} \right) x_{Di} + \left( \frac{1 + \frac{B}{D}}{r+1} \right) \left( \frac{k_f}{k_{f,\text{ref}}} \right) \left( \frac{Da}{N_T} \right) \sum_{j=1}^m \left( x_{j,3}^2 - \frac{x_{j,1} x_{j,2}}{K} \right) = 0 \quad (i=1, 2) \quad (\text{C2})$$

$$x_{n+1,i} - \left( \frac{s}{s+1} \right) y_{n,i} - \left( \frac{1}{s+1} \right) x_{Bi} + \left( \frac{1 + \frac{D}{B}}{s+1} \right) \left( \frac{k_f}{k_{f,\text{ref}}} \right) \left( \frac{Da}{N_T} \right) \sum_{j=1}^n \left( x_{j,3}^2 - \frac{x_{j,1} x_{j,2}}{K} \right) = 0 \quad (i=1, 2). \quad (\text{C3})$$

The total holdup,  $H_T$  is distributed equally on all stages and  $N_T$  is the total number of stages in the column. Also the reflux ratio, reboil ratio, and  $D/B$  are related by the energy balance in Eq. 11.

The location of the saddle fixed points is central to the determination of the distillation limit at minimum reflux. Therefore, on investigating the behavior of the saddle fixed points branches of the rectifying and stripping sections with  $Da$ , we find

1. At  $Da=0$ , the saddle fixed points for the rectifying and stripping sections are located at the light-intermediate and intermediate-heavy edges of the triangular phase space.

2. For  $0 < Da < \delta$ , the saddle fixed points travel continuously from the edges of the composition triangle to the equilibrium curve ( $\delta < 0.1$ ).

3. For  $Da \geq \delta$ , the saddle fixed points remain on the equilibrium curve.

To calculate the location of these saddle fixed points we require a very high numerical precision (greater than quad precision for  $0 < Da < \delta$ ). Moreover, the fixed points move very quickly onto the equilibrium curve and remain there ( $Da \geq \delta$ ). This range ( $Da \geq \delta$ ) is in fact covered very well by the model for which  $Da$  is defined by Eq. 10. Therefore, considering the computational expenditure involved in locating the saddle fixed points and the corresponding small gain-continuity in the  $0 < Da < \delta$  range, the total holdup formulation does not seem an attractive proposition for the determination of the distillation limit at minimum reflux.

*Manuscript received July 6, 1999, and revision received Dec. 9, 1999.*